

## ORIGINAL

# Evaluation of the components of mediastinal cystic lesions using imaging techniques

Koichiro Kajiu<sup>1,3</sup>, Shoichiro Takao<sup>2</sup>, Naoko Kawano<sup>2</sup>, Toru Sawada<sup>1</sup>, Mitsuhiro Tsuboi<sup>1</sup>, Hiroaki Toba<sup>1</sup>, Mitsuteru Yoshida<sup>1</sup>, Hiromitsu Takizawa<sup>1</sup>, Akira Tangoku<sup>1</sup>, and Kazuya Kondo<sup>4</sup>

<sup>1</sup>Department of Thoracic, Endocrine, and Oncological Surgery, Graduate School of Biomedical Sciences, Tokushima University, Tokushima, Japan; <sup>2</sup>Department of Diagnostic Radiology, Graduate School of Biomedical Sciences, Tokushima University, Tokushima, Japan; <sup>3</sup>Department of Thoracic Center, Urasoe General Hospital, Okinawa, Japan; <sup>4</sup>Department of Oncological Medical Services, Graduate School of Biomedical Sciences, Tokushima University, Tokushima, Japan

**Abstract : Objective :** To identify and differentiate patients with mediastinal cysts from those with cystic tumors requiring surgery. **Methods :** A total of 36 patients with mediastinal cystic lesions were enrolled. The patients were separated into two groups based on pathological findings : those with mediastinal cysts (n=23) and those with mediastinal tumors (n=13). The cystic components were measured using imaging parameters including mean computed tomography (CT) value, apparent diffusion coefficient (ADC), T1 signal intensity ratio (T1SI-ratio), and T2 signal intensity ratio (T2SI-ratio), acquired from magnetic resonance imaging (MRI) ; and standardized maximum uptake value (SUVmax) from <sup>18</sup>F-fluorodeoxyglucose positron emission tomography/computed tomography (<sup>18</sup>F-FDG PET/CT). Both groups were statistically compared. **Results :** Comparative parameters between the cysts and tumors revealed the following ratios : CT value, 40.9±21.2 versus (vs) 24.8±12.9 (p = 0.019) ; SUVmax, 1.18±0.50 vs 4.32±3.52 (p = 0.003) ; ADC, 3.46±0.96 vs 2.68±0.74 (p = 0.022) ; T1SI-ratio, 1.06±0.60 vs 1.35±0.92 (p = 0.648) ; T2SI-ratio, 5.40±1.80 vs 4.33±1.58 (p = 0.194). However, there was no correlation between FDG uptake and ADC value. **Conclusions :** SUVmax from <sup>18</sup>F-FDG PET/CT and ADC derived from MRI were effective in facilitating preoperative diagnosis to differentiate mediastinal cysts from tumors. However, these examinations may be complementary to one another, not dominant. *J. Med. Invest.* 66 : 106-111, February, 2019

**Keywords :** Mediastinal cystic lesions, <sup>18</sup>F-FDG PET/CT, Magnetic resonance imaging

## INTRODUCTION

Mediastinal cystic lesions are sometimes identified on chest computed tomography (CT). It has been reported that mediastinal cystic lesions comprise 37.9% of bronchogenic cysts, 24.1% of hydatid cysts, 13.8% of benign cystic teratomas, 10.3% of pericardial cysts, 5.3% of thymic cysts, 5.3% of enteric cysts, and 5.3% of lymphangiomas (1). Surgery is required in cases of thymoma with coagulation necrosis, teratoma with cystic components, and infected bronchogenic cysts. However, patients with simple mediastinal cysts, such as thymic and pericardial cysts, usually do not require surgery and can simply be managed with regular follow-up.

However, pre-operative diagnosis of mediastinal simple cysts is sometimes difficult (2). It has been reported that small intrathymic cysts (< 3 cm) are often misdiagnosed, and unnecessary invasive surgeries are performed (3). Therefore, it is necessary to use appropriate imaging tools to distinguish simple serous cysts from tumors with necrosis.

Imaging tools for mediastinal lesions include CT, magnetic resonance imaging (MRI), and <sup>18</sup>F-fluorodeoxyglucose positron emission tomography/computed tomography (<sup>18</sup>F-FDG PET/CT). Mediastinal cysts are usually differentiated from mediastinal cystic tumors based on imaging characteristics including lesion

shape, and thickness and irregularity of the lesion walls. Morphology is the most important feature for preoperative diagnosis. However, differential diagnosis using mass shape and wall findings are somewhat subjective. Therefore, objective diagnostic criteria using quantitative analysis such as CT attenuation value (CT value) of unenhanced CT, signal intensity (SI) of MRI, apparent diffusion coefficient (ADC) value of diffusion-weighted MRI, or standard uptake value (SUV) of <sup>18</sup>F-FDG PET should be considered to facilitate preoperative diagnosis based on morphology. In the present study, we assessed the importance and utility of the above-mentioned imaging tools and values in distinguishing mediastinal cysts from cystic tumors, observing only the cystic components of the lesions and not the solid parts.

## PATIENTS AND METHODS

### Subjects

A total of 36 patients (11 men, 25 women) who underwent surgery after being diagnosed with a mediastinal cystic mass and were treated at the Tokushima University Hospital (Tokushima Prefecture, Japan) between February 2008 and November 2016, were enrolled in this study. Patients underwent CT, MRI, and/or <sup>18</sup>F-FDG PET/CT before surgery. The pathological diagnoses of patients with cystic lesions are listed in Table 1 and Table 2. Findings from acquired images of these patients were then retrospectively analyzed. The study protocol was approved by the Institutional Review Board of the Tokushima University Hospital (approval number 2949), and conformed to the Declaration of

Received for publication April 17, 2018 ; accepted October 1, 2018.

Address correspondence and reprint requests to Shoichiro Takao, MD, PhD, Assistant Professor, Department of Diagnostic Radiology, Graduate School of Biomedical Sciences, Tokushima University, Tokushima, 770-8503, Japan and Fax : +81-88-633-9865.

Table1. The patients list with mediastinal cysts

case	age	gender	diagnosis	CT	PET-CT	MRI		
				CT value (mean)	SUV max	ADC value	T1SI-ratio	T2SI-ratio
1	55	M	thymic cyst	10.6	0.6	3.8	0.4	6.2
2	74	F	thymic cyst	N.A.	N.A.	4.7	0.5	5.0
3	68	F	thymic cyst	58.9	N.A.	4.1	1.1	5.6
4	59	M	thymic cyst	N.A.	N.A.	3.6	0.7	8.6
5	65	F	thymic cyst	47.8	1.7	0.8	3.0	8.6
6	63	F	thymic cyst	71.1	1.2	N.A.	N.A.	N.A.
7	75	F	thymic cyst	42.2	0.8	4	0.9	3.9
8	69	F	thymic cyst	48.2	N.A.	N.A.	1.2	7.4
9	68	F	thymic cyst	36.1	0.8	3.3	1.4	3.4
10	57	F	thymic cyst	61.3	0.6	N.A.	N.A.	N.A.
11	68	M	mediastinal cyst	59.6	1.9	1.8	N.A.	3.0
12	68	F	thymic cyst	67.2	0.6	2.8	1.5	6.6
13	60	M	thymic cyst	61.3	N.A.	3.6	1.6	5.0
14	50	F	thymic cyst	50.3	1.5	3.3	N.A.	6.4
15	78	F	thymic cyst	55.6	1.1	3.2	1.3	2.8
16	86	F	pericardial cyst	12.3	N.A.	4.8	0.9	7.5
17	65	F	thymic cyst	50	N.A.	4	1.2	5.4
18	51	M	pericardial cyst	3.3	1.3	3.9	0.4	6.2
19	78	F	thymic cyst	3.6	N.A.	4.6	0.5	2.5
20	43	F	Müllerian ductic cyst	5.9	N.A.	2.4	0.5	4.8
21	59	M	bronchogenic cyst	41.3	N.A.	3.4	1.1	5.4
22	48	M	bronchogenic cyst	41	N.A.	3.6	1.0	3.2
23	61	M	bronchogenic cyst	31.3	2.0	N.A.	N.A.	N.A.

\*N.A. was not performed examination

\* Fig.1 showed case15 as representative

Table2. The patients list with mediastinal tumors

case	age	gender	diagnosis	CT	PET/CT	MRI		
				CT value (mean)	SUV max	ADC value	T1SI-ratio	T2SI-ratio
1	20	F	mature cystic teratoma	22.4	2.1	N.A.	1.6	5.8
2	84	F	B1/B2 thymoma	44.7	N.A.	2.6	N.A.	2.9
3	42	M	thymoma	26.7	N.A.	1.8	0.5	3.9
4	68	F	thymic cancer	33.5	N.A.	3	0.9	2.4
5	80	F	micronodular thymoma	7.5	0.6	4.1	3.5	6.6
6	46	F	mature cystic teratoma	8.8	5.4	3.1	N.A.	6.8
7	47	F	mature cystic teratoma	7.3	1.4	1.5	1.1	5.1
8	40	F	B2 thymoma	32.5	2.2	2.5	N.A.	3.8
9	68	M	cystic teratoma	25	2.5	N.A.	N.A.	N.A.
10	38	F	B1/B2 thymoma	48	13.0	N.A.	N.A.	N.A.
11	65	F	A thymoma	28.5	3.1	2.3	1.1	2.1
12	65	M	B1 thymoma	27.1	5.4	3.2	0.8	3.8
13	27	F	mature cystic teratoma	10.2	7.5	N.A.	N.A.	N.A.

\*N.A. was not performed examination

Helsinki.

*Imaging acquisition and analysis*

<sup>18</sup>F-FDG PET/CT: Of the 36 patients, 20 underwent <sup>18</sup>F-FDG PET/CT before the surgery. The patients were confirmed to have blood glucose levels < 150 mg/dl, and were intravenously injected with 3.7 MBq/kg of <sup>18</sup>F-FDG. One hour after <sup>18</sup>F-FDG injection, the patients were examined using a PET/CT scanner (Aquiduo;

Toshiba Medical Systems Corporation, Tochigi, Japan), which was replaced with a new PET/CT scanner (GE Healthcare, Chicago, United States) in April 2015. For examination using the new PET/CT scanner, patients were intravenously injected with 3.0 MBq/kg of <sup>18</sup>F-FDG. Images from each patient were acquired from the top of the head to the middle of the thigh. CT images were acquired using a 16-slice multi-detector row CT (MDCT) scanner under free breathing conditions, and reconstructed using a slice thickness

of 2 mm. Fusion images between attenuation-corrected <sup>18</sup>F-FDG PET and non-contrast CT images were generated using commercially available software (Aquarius NET Viewer Version 4.4.11.265 ; TeraRecon Inc., San Mateo, CA, USA). Analysis of <sup>18</sup>F-FDG PET images was performed using the same software. Each cystic component of the mediastinal lesions was segmented in the CT image at its maximum diameter by manually drawing a polygonal region of interest (ROI) excluding intralesional calcifications, adjacent mediastinal fat, and normal structures including the great vessels, myocardium, and lungs. The same ROI was then applied to the fusion image. Segmentation of the mass was performed by a certified radiologist (ST [17 years' experience in diagnostic radiology]). Mean CT attenuation values and maximum SUV (SUVmax) of the cystic components of mediastinal lesions were then calculated (Figure 1a).

**MRI :** Of the 36 patients, 28 underwent MRI examination. Patients were examined using a 1.5 Tesla scanner (Signa Excite HD ; GE Healthcare, Buckinghamshire, UK). Fast spin echo (FSE) or gradient echo T1-weighted images (T1WIs), FSE T2-weighted images (T2WIs), and diffusion-weighted images (DWIs) were obtained. All T1WIs, T2WIs, and DWIs were acquired in axial view. MRI imaging parameters, including repetition time (TR), echo time (TE), image matrix, field of view, and slice thickness/gap, were different for each case and depended on the size or location of the mass. DWIs were acquired under free breathing conditions with an echo-planar imaging pulse sequence, 'b' values (b = 0, 800), and free breathing. The SI of each mediastinal mass and calculated apparent diffusion coefficient (ADC) were analyzed using an imaging workstation (SYNAPSE VINCENT Version 4.4 ; Fujifilm Medical Co., Tokyo, Japan). For T1WIs and T2WIs, all cystic components of the mediastinal lesions were segmented at the level of maximum diameter by manually drawing a polygonal ROI, excluding adjacent mediastinal fat and normal structures, including the great vessels, myocardium, and lungs. In addition, an oval-shape ROI was applied to the nearby skeletal muscles, including the pectoralis major, latissimus dorsi, or paraspinal muscles, to obtain a reference for the signal intensity. Segmentation of the mass was then performed by the same certified radiologist mentioned above. T1 signal intensity ratio (T1SI-ratio) defined as T1SI (lesion)/T1SI (muscle) and the T2

signal intensity ratio (T2SI-ratio) defined as T2SI (lesion)/T2SI (muscle) were calculated (Figure 1b/1c). To analyze ADC, the ROI was set to the mass by referring to T1WIs, T2WIs, or b0 images. Finally, an average ADC value was calculated using plug-in software (ADC Map) of the above-mentioned imaging workstation (Figure 1 d).

**Conventional CT :** Unenhanced conventional CT images were acquired using two different 16-slice MDCT scanners (Aquilion16 ; Toshiba Medical Systems Corporation, Tochigi, Japan ; SOMATOM Sensation 16 ; Siemens, Erlangen, Germany) as well as a 320-slice MDCT scanner (Aquilion one ; Toshiba Medical Systems Corporation, Tochigi, Japan) under breath-holding conditions. CT images were reconstructed using a slice thickness of 1 mm. Each cystic component of the mediastinal lesions was segmented in the CT image at the level of maximum diameter by manually drawing a polygonal ROI excluding intralesional calcifications, adjacent mediastinal fat, and normal structures such as the great vessels, myocardium, and lungs. Segmentation of the mass was performed by the same certified radiologist mentioned above. The CT attenuation value (CT value) of the mass was calculated using commercially available software (Aquarius NET Viewer Version 4.4.11.265 ; TeraRecon Inc., San Mateo, CA, USA) (Figure 1a).

*Statistical analysis*

Results are expressed as mean ± standard deviation. The non-parametric Mann-Whitney U test was used to compare data that were not normally distributed. Statistical analyses were performed using R 3.2.2 (R Project for Statistical Computing, Vienna, Austria). In CT value analysis, values from conventional CT were preferentially used for analysis for patients who underwent both conventional CT and <sup>18</sup>F-FDG PET/CT. For patients who did not undergo conventional unenhanced CT, CT values from <sup>18</sup>F-FDG PET/CT were used for analysis.

*Reproducibility*

Another radiologist (NK [7 years' experience in radiology]) measured the same cases to confirm reproducibility using the interclass correlation coefficient (inter-ICC).

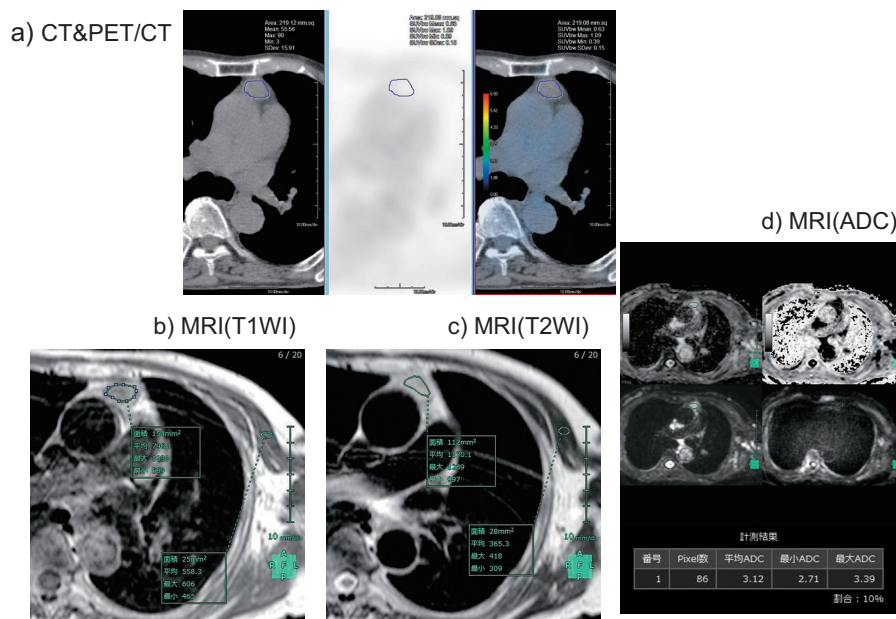


Figure 1. The method of measuring each parameter in a representative case (case 15).

RESULTS

Characteristics of the groups, as revealed by CT, MRI, and <sup>18</sup>F-FDG PET/CT images

There were 23 cases involving mediastinal cysts, including sixteen thymic cysts, three bronchogenic cysts, two pericardial cysts, a thoracic benign cyst, and a Mullerian duct cyst. There were 13 cases of mediastinal cystic tumors comprising seven thymomas with necrosis, five mature teratomas, and one thymic cancer with necrosis. Comparative measurements of different parameters between the mediastinal cyst group and mediastinal cystic tumor group, respectively, revealed the following : On CT, CT value, 40.9 ± 21.2 vs 24.8 ± 12.9 Hounsfield units (HU) (p = 0.019) ; SUVmax of <sup>18</sup>F-FDG PET/CT, 1.18 ± 0.50 vs 4.32 ± 3.52 (p = 0.003) ; and on MRI, ADC, 3.46 ± 0.96 vs 2.68 ± 0.74 (×10<sup>3</sup> mm<sup>2</sup>/s) (p = 0.022), T1SI-ratio, 1.06 ± 0.60 vs 1.35 ± 0.92 (p = 0.648), T2SI-ratio, 5.40 ± 1.80 vs 4.33 ± 1.58 (p = 0.194) (Table 3).

The average SUVmax in the mediastinal cysts group was significantly lower than that of the mediastinal cystic tumors group (Figure 2). Receiver operating characteristic (ROC) curve analysis revealed a cut-off value of 2.1. If the SUVmax in the mediastinal cysts was < 2.1, the sensitivity was 100%, and the specificity was 80.0% for differentiating from mediastinal cystic tumors. Thus, the SUVmax of <sup>18</sup>F-FDG PET/CT was an effective imaging technique to distinguish mediastinal cysts from mediastinal cystic tumors. Additionally, the average value of ADC with MRI in the mediastinal cysts tended to be higher than that of mediastinal cystic tumors. The ROC curve revealed a cut-off value of 3.3. If the ADC in the mediastinal cysts was > 3.3, the sensitivity was 88.8% and the specificity was 73.7% for differentiating mediastinal cysts from mediastinal cystic tumors (Figure 2).

ADC value and SUVmax demonstrated significant differences for the diagnosis of mediastinal cystic masses. However, there

was no correlation between SUVmax and ADC value in each case (Figure 3) ; the coefficient of determination (R<sup>2</sup>) was 0.024. Average values for T1SI-ratio and T2SI-ratio with MRI between the mediastinal cysts and mediastinal cystic tumors were not statistically different.

Finally, the average CT value in mediastinal cysts were found to be higher than that of mediastinal cystic tumors. There was a positive correlation between the average CT value within the ROI and the T1SI-ratio in mediastinal cysts, except for bronchogenic cysts, which exhibited milky white fluid, with a correlation coefficient of 0.6538 (p = 0.01) (Figure 4). Surgical findings revealed that mediastinal cysts, except bronchogenic cysts, exhibited light bloody fluid in 9 of 14 (64.3%) cases.

DISCUSSION

The present retrospective study focused on the cystic components of lesions, and revealed that <sup>18</sup>F-FDG PET/CT was a useful imaging tool to distinguish mediastinal serous cysts from mediastinal cystic tumors. The mean SUVmax was 1.18 ± 0.50 vs 4.32 ± 3.52 in mediastinal cysts and mediastinal cystic tumors, respectively (p=0.003). The sensitivity of <sup>18</sup>F-FDG PET/CT was 100% and the specificity was 80.0%, if SUVmax was < 2.1.

It has been reported that SUVmax of <sup>18</sup>F-FDG PET/CT indicates the degree of malignancy in thymic epithelial tumors (5, 6), and inflammation such as in abscesses (7). There have been no reports suggesting that the cells present in mediastinal cysts under non-inflammatory conditions exhibit glucose uptake. Therefore, it appears clear that uptake of <sup>18</sup>F-FDG would not be expected to occur in mediastinal cysts.

ADC values on DWIs are useful in distinguishing non-neoplastic cysts from solid masses. This is because the ADC values of non-

Table3. Patients characteristics with mediastinal cystic mass in CT, <sup>18</sup>F-FDG PET/CT, and MRI examinations.

	mediastinal cysts (n=23)	mediastinal tumors (n=13)	p-value	Inter-ICC
age	63.8 ± 10.3	53.1 ± 19.2		
gender (M : F)	8 : 15	3 : 10		
diagnosis	thymic cyst (n=16) bronchogenic cysts (n=3) pericardial cysts (n=2) thoracic cyst (n=1) Mullerian duct cyst (n=1)	thymoma (n=7) mature teratoma (n=5) thymic cancer (n=1)		
<b>CT</b>				
CT value (H.U.)	40.9 ± 21.2 (n=21)	24.8 ± 12.9 (n=13)	<u>0.019</u>	0.985
<b><sup>18</sup>F-FDG PET/CT</b>				
SUVmax	1.18 ± 0.50 (n=12)	4.32 ± 3.52 (n=10)	<u>0.003</u>	0.824
<b>MRI</b>				
ADC value (x10 <sup>-3</sup> mm <sup>2</sup> /sec)	3.46 ± 0.96 (n=19)	2.68 ± 0.74 (n=9)	<u>0.022</u>	0.693
T1SI-ratio	1.06 ± 0.60 (n=18)	1.35 ± 0.92 (n=7)	0.648	0.904
T2SI-ratio	5.40 ± 1.80 (n=20)	4.33 ± 1.58 (n=10)	0.194	0.535

\*Inter-ICC : interclass correlation coefficient

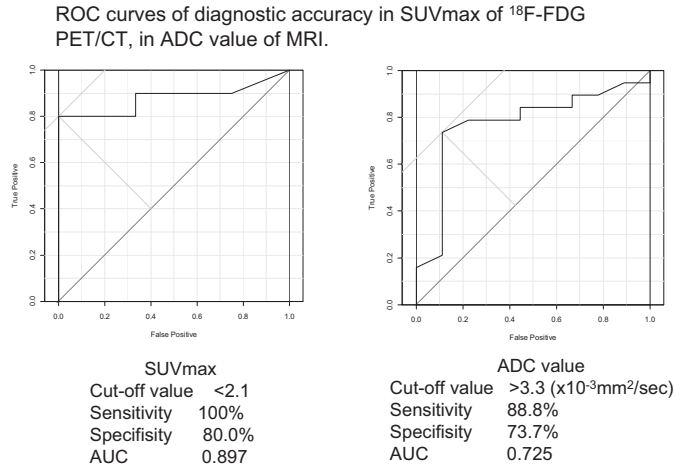


Figure 2. Receiver operating characteristic (ROC) curves of the standardized maximum uptake value (SUVmax) of <sup>18</sup>Fluorodeoxyglucose positron emission tomography/computed tomography (<sup>18</sup>F-FDGPET/CT) and the apparent diffusion coefficient (ADC) value of magnetic resonance imaging (MRI).

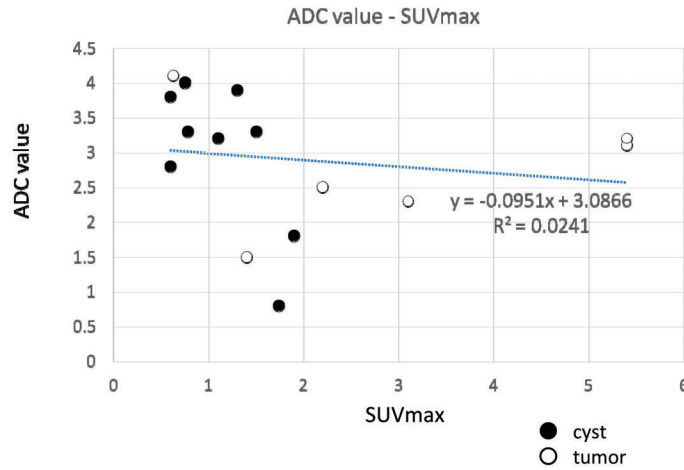


Figure 3. The correlation between apparent diffusion coefficient (ADC) value and the standardized maximum uptake value (SUVmax) in each case. The coefficient of determination ( $R^2$ ) was 0.024.

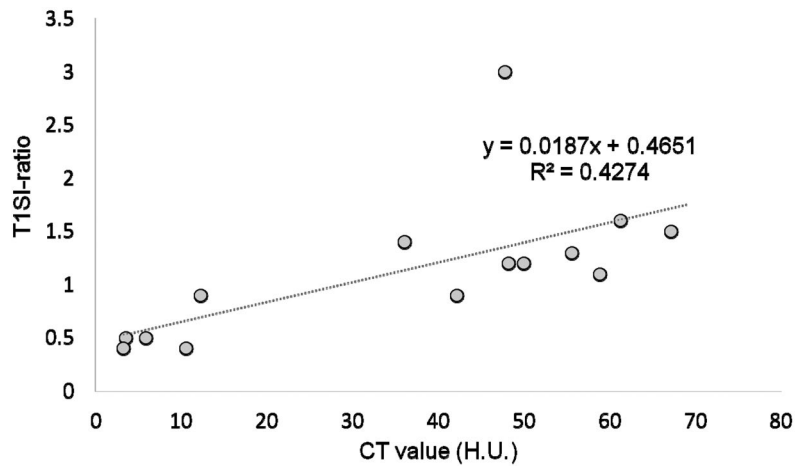


Figure 4. The relationship between mean computed tomography (CT) values within the region of interest (ROI) and T1-signal intensity (T1SI) ratio in mediastinal cysts. A positive correlation was obtained between average CT values within the ROI and the T1SI-ratio in mediastinal cysts.

neoplastic cysts are significantly higher than that of solid masses (8). ADC values have also been previously investigated in an attempt to distinguish between benign and malignant tumors in the head, neck, thyroid, and mediastinum, as well as pulmonary lesions (9-13). Under normal conditions, water molecules move freely in the extracellular compartment. This movement of water molecules may be affected by the presence of proteins, inflammatory cells, and tumor cells in the environment. Generally, ADC values are inversely proportional to protein concentration and cellular density. The ADC value in DWIs tends to be lower due to restriction of the microscopic movement of water molecules caused by bacteria, inflammatory cells, cellular debris, protein complexes, and tumor cells (13). It has also been reported that DWI on MRI can differentiate benign lesions from malignant tumors, even among cystic lesions (14). In the present study, we found that the ADC values were statistically higher ( $p=0.022$ ) in mediastinal cysts, even compared with the cystic components of mediastinal cystic tumors.

In the present study, the CT values were found to be higher in mediastinal cysts compared with mediastinal cystic tumors. In CT, serous fluid is usually recognized as a lower density area compared with the mucinous fluid area. However, the results from our study were the opposite of what we expected. Surgical findings revealed that the fluid content of the mediastinal cysts were light bloody in 9 of 14 (64.3%) cases. In addition, there was a positive correlation between the mean CT value within ROI and T1SI-ratio in mediastinal cysts. It has been established that fat, hematoma, mucin, and high-density lipoprotein exhibit high intensity on T1 WI. In this study, it may be possible that mediastinal cysts exhibited high intensity on T1WI due to intracystic blood cells. Naturally, the cause of high CT values in the patients was not limited to intracystic bleeding; other factors were also believed to play a role.

We verified the reproducibility of the measurements performed by the other radiologist using the inter-ICC. The inter-ICC was 0.985 for CT value, 0.824 for SUVmax, 0.693 for ADC, 0.904 for T1SI, and 0.535 for T2SI. Only T2SI was affected by observer bias; however, CT value, SUVmax, and T1SI were essentially reproducible. Inter-ICC values  $> 0.6$  are considered to reflect high reproducibility; therefore, we believe there was no observer bias regarding ADC and SUVmax.

There were a few limitations to our study, the first of which was the small number of cases of mediastinal cysts and mediastinal cystic tumors. Second, we acknowledge that there may have been selection bias in this retrospective study because only surgical cases were enrolled and used in the final pathological diagnosis. Usually, patients with typical mediastinal cysts are diagnosed based on observations using imaging tools, and do not necessarily undergo surgical treatment. Third, measurement bias for SUVmax was possible in a portion of patients because the PET/CT scanner in the Tokushima University Hospital was replaced in April 2015. Fourth, CT value was measured using conventional CT or PET/CT. There may have been measurement bias for the CT value because CT imaging in PET/CT was performed using low-dose X-rays under spontaneous respiration.

There have been only a few previous studies that have compared mediastinal cystic component images obtained using different imaging tools. Based on our findings, we conclude that quantitative evaluation using  $^{18}\text{F}$ -FDG PET/CT and/or MRI imaging including DWIs can facilitate preoperative diagnosis based on morphology, and avoid unnecessary surgical procedures in patients with mediastinal cysts.

## GRANT SUPPORT

This study was not supported by any grant.

## REFERENCES

1. Aydin Y, Oqul H, Turkyilmaz A, Eroqlu A : Surgical treatment of mediastinal cysts : report on 29 cases. *Acta Chir Belg* 112 : 281-286, 2012
2. Gochi F, Omasa M, Yamada T, Sato M, Menju T, Aoyama A, Sato T, Chen F, Sonobe M, Date H : Factors affecting the preoperative diagnosis of anterior mediastinal cysts. *Gen Thorac Cardiovasc Surg* 63(6) : 349-353, 2015
3. Li X, Han X, Sun W, Wang M, Jing G, Zhang X : Preoperative misdiagnosis analysis and accurate distinguish intrathymic cyst from small thymoma on computed tomography. *J Thorac Dis* 8 : 2086-2092, 2016
4. Ackman JB, Verzosa S, Kovach A, Louissaint A, Jr, Lanuti M, Wright CD, Shepard JO, Halpem EF : High rate of unnecessary thymectomy and its cause. Can computed tomography distinguish thymoma, lymphoma, thymic hyperplasia, and thymic cysts?. *Eur J Radiol* 84(3) : 524-533, 2015
5. Kitami A, Sano F, Ohashi S, Suzuki K, Uematsu S, Suzuki T, Kadokura M : The usefulness of positron-emission tomography findings in the management of anterior mediastinal tumors. *Ann Thorac Cardiovasc Surg* 23(1) : 26-30, 2017
6. Kumar A, Regmi SK, Dutta R, Kumar R, Gupta SD, Das P, Halanaik T : Characterization of thymic masses using  $^{18}\text{F}$ -FDG PET-CT. *Ann Nucl Med* 23(6) : 569-577, 2009
7. Treglia G, Bertagna F, Muoio B, Giovannella L :  $^{18}\text{F}$ -FDG PET/CT detected a septic focus corresponding to a small periurethral abscess in a patient with bacteremia due to *Enterococcus faecium*. *Rev Esp Med Nucl Imagen Mol* 34(3) : 209-210, 2015
8. Shin KE, Yi CA, Kim TS, Lee HY, Choi YS, Kim HK, Kim J : Diffusion-weighted MRI for distinguishing non-neoplastic cysts from solid masses in the mediastinum : problem-solving in mediastinal masses of indeterminate internal characteristics on CT. *Eur Radiol* 24(3) : 677-684, 2014
9. Srinivasan A, Dvorak R, Perni K, Rohrer S, Mukherji SK : Differentiation of benign and malignant pathology in the head and neck using 3T apparent diffusion coefficient values : early experience. *Am J Neuroradiol* 29(1) : 40-44, 2008
10. Abdel Razek AA, Gaballa G, Elhawary G, Megahed AS, Hafez M, Nada N : Characterization of pediatric head and neck masses with diffusion-weighted MR imaging. *Eur Radiol* 19(1) : 201-208, 2008
11. Razek AA, Sadek AG, Kombar OR, Elmahdy TE, Nada N : Role of apparent diffusion coefficient values in differentiation between malignant and benign solitary thyroid nodules. *Am J Neuroradiol* 29(3) : 563-568, 2008
12. Abdel Razek AAK, Soliman N, Elashery R : Apparent diffusion coefficient values of mediastinal masses in children. *Eur J Radiol* 81(6) : 1311-1314, 2012
13. Liu H, Liu Y, Yu T, Ye N : Usefulness of diffusion-weighted MR imaging in the evaluation of pulmonary lesions. *Eur Radiol* 20(4) : 807-815, 2010
14. Bukte Y, Paksoy Y, Genc E, Uca AU : Role of diffusion-weighted MR in differential diagnosis of intracranial cystic lesions. *Clin Radiol* 60(3) : 375-383, 2005

## CONFLICT OF INTEREST

The authors have no conflicts of interest to declare.